VOL. 12, NO. 19, OCTOBER 2017 ISSN 1819-6608
ARPN Journal of Engineering and Applied Sciences

www.arpnjournals.com

THERMAL-DIFFUSION AND DIFFUSION-THERMO EFFECTS ON MHD FLOW THROUGH POROUS MEDIUM PAST AN EXPONENTIALLY ACCELERATED INCLINED PLATE WITH VARIABLE TEMPERATURE

Siva Reddy Sheri[1] and Prasanthi Modugula[2]
[1]Department of Mathematics, GITAM University, Hyderabad Campus, Telangana, India
[2]Department of Mathematics, CMRTC, Kandlakoya, Medchal, Telangana, India
E-Mail: sreddy7@yahoo.co.in

ABSTRACT

The aim of the present paper is an investigation of thermal-diffusion and diffusion-thermo effects on MHD flow through porous medium past an exponentially accelerated inclined plate with variable temperature. The governing non-linear partial differential equations are transformed into a system of coupled non-linear ordinary differential equations using similarity transformations. A robust finite element method (FEM) has been adopted to obtain the solution of the transformed flow equations with corresponding initial and boundary conditions. Extensive discussion of the finite element formulation, convergence and validation is provided. The influence of physical parameters on dimensionless velocity, temperature and concentration are presented graphically to illustrate interesting features of the solutions. The effect of flow pertinent parameters on skin friction, Nusselt number and Sherwood number are discussed and presented in tabular form. Finally, a qualitative comparison has been made between the present work and previous published result, found that there is an excellent agreement between the results exists.

Keywords: MHD, thermal-diffusion, diffusion-thermo, inclined plate, FEM.

INTRODUCTION

In the above mentioned works, the diffusion-thermo (Dufour) and the thermal-diffusion (Soret) terms were not taken into account in the energy and concentration equations respectively. But when the heat and mass transfer occur simultaneously in a moving fluid, the relations between the fluxes and driving potentials are of a more intricate nature. It is found that a heat flux can be generated not only by temperature gradients but by composition gradients as well. The heat flux that occurs due to composition gradient is called the Dufour effect or diffusion-thermo effect. On the other hand the flux of mass caused due to temperature gradient is known as the Soret effect or the thermal-diffusion effect. The experimental investigation of the thermal-diffusion effect on mass transfer related problems was first done by Charles Soret in 1879. Hence this thermal-diffusion is known as the Soret effect in honour of Charles Soret. In general the Soret and Dufour effects are of a smaller order of magnitude than the effects described in Fourier's or Fick's law and are often neglected in heat and mass transfer processes. Though these effects are quite small, certain devices can be arranged to produce very steep temperature and concentration gradients so that the separation of components in mixtures are affected. Postelnicu [1] analyzed the simultaneous heat and mass transfer by natural convection from a vertical flat plate embedded in an electrically-conducting fluid saturated porous medium using the Darcy Boussinesq model in the presence of Dufour and Soret effects. Ramzan *et al*. [2] examined three dimensional boundary layer flow of a viscoelastic nanofluid with Soret and Dufour effects. Nayak *et al*. [3] analyzed Soret and Dufour effects on mixed convection unsteady MHD boundary layer flow over stretching sheet in porous medium with chemically reactive species. Tai Bo-Chen and Char Ming [4] have studied Soret and Dufour effects on free convection flow of non-Newtonian fluids along a vertical plate embedded in a porous medium with thermal radiation. Mohammad Ali and Mohammad Shah Alam [5] have investigated Soret and Hall Effect on MHD flow, heat and mass transfer over a vertical stretching sheet in a porous medium due to heat generation.

The conjugate phenomena of heat and mass transfer flows in an exponentially accelerated inclined plate embedded in a porous medium has many engineering and geophysical applications such as chemical industry, geothermal reservoirs, drying of porous solids, thermal insulation, enhanced oil recovery, MHD power generators, packed-bed catalytic reactors, cooling of nuclear reactors and underground energy transport. Heat and mass transfer in wet porous media take place coupled in a complicated way. The varied structure of the solid matrix widely in shape. There is, in general, a distribution of void sizes, and the structures may also be locally irregular. Energy transport in such a medium occurs in all phases by conduction. Mass transport occurs within voids of the medium. The voids in an unsaturated state are filled with a liquid partially filled, while the remaing voids are filled with some gas. The concept that no hygroscopic fiber is a common misapprehension (i.e., those of low intrinsic for moisture vapor) will automatically produce a hydrophobic fabric. Recently, Seth *et al.* [6] presented heat and mass transfer effects on unsteady MHD natural convection flow of a chemically reactive and radiating fluid through a porous medium past a moving vertical plate with arbitrary ramped temperature. Siva Reddy and Anjan Kumar [7] have presented Finite element analysis of heat and mass

transfer past an impulsively moving vertical plate with ramped temperature. Rudraswamy and Gireesha [8] studied the Influence of chemical reaction and thermal radiation on MHD boundary layer flow and heat transfer of a nanofluid over an exponentially stretching sheet. Siva Reddy *et al*. [9] have explored Heat and mass transfer effects on MHD natural convection flow past an infinite inclined plate with ramped temperature. Anand Rao *et al.* [10] have discussed Radiation effects on an unsteady MHD vertical porous plate in the presence of homogeneous chemical reaction. Pattnaik *et al*. [11] analyzed radiation and mass transfer effects on MHD flow through porous medium past an exponentially accelerated inclined plate with variable temperature.

The study of fluid flows and heat transfer through porous medium has attracted much attention recently. This is primarily because of numerous applications of flow through porous medium, such as storage of radioactive nuclear waste materials transfer, separation processes in chemical industries, filtration, transpiration cooling, transport processes in aquifers, ground water pollution, etc. Examples of natural porous media are beach sand, sandstone, limestone, rye bread, wood, the human lung, bileduct, gall bladder with stones and in small blood vessels. In some pathological situations, the distribution of fatty cholesterol and artery clogging blood clots in the lumen of coronary artery can be considered as equivalent to a porous medium. Comprehensive literature surveys concerning the subject of porous media can be found in the most recent books by Nield and Bejan [12], Vafai [13], Pop and Ingham [14]. Das *et al*. [15] examined the mass transfer effects on MHD flow and heat transfer past a vertical porous plate through a porous medium under oscillatory suction and heat source. Anand Rao *et al.* [16] have analyzed Chemical reaction effects on an unsteady magneto hydrodynamics (MHD) free convection fluid flow past a semi-infinite vertical plate embedded in a porous medium with heat absorption.

The present study is to investigate the combined effects of thermal-diffusion and diffusion-thermo effects on MHD flow through porous medium past an exponentially accelerated inclined plate with variable temperature. The paper is organized as follows: Section 1 presents the literature review related to the research subject; section 2 describes the formulation of the problem; section 3 describes the adopted methodology in this research; section 4 describes the validations of numerical results; the results and discussion are then introduced in section 5; and section 6 presents some concluding remarks.

Formulation of the Problem

In the present work we consider the unsteady uniform MHD free convective flow of a viscous, incompressible and radiating fluid past an accelerated inclined infinite plate with variable temperature embedded in a saturated porous medium. The x' axis is taken along the plate with the angle of inclination α to the vertical and the $y'-$ axis is taken normal to the plate. A uniform magnetic field of strength B_0 is applied in the direction perpendicular to the plate. The induced magnetic field is neglected as the magnetic Reynolds number of the flow is very small. Initially, it is assumed that the plate and the surrounding fluid are at the same temperature T'_∞ and concentration C'_∞. At time $t' > 0$, the plate is exponentially accelerated with a velocity $u' = u_0 \exp(a't')$ in its own plate. At the same time the temperature and concentration level are also raised or lowered linearly with time t.

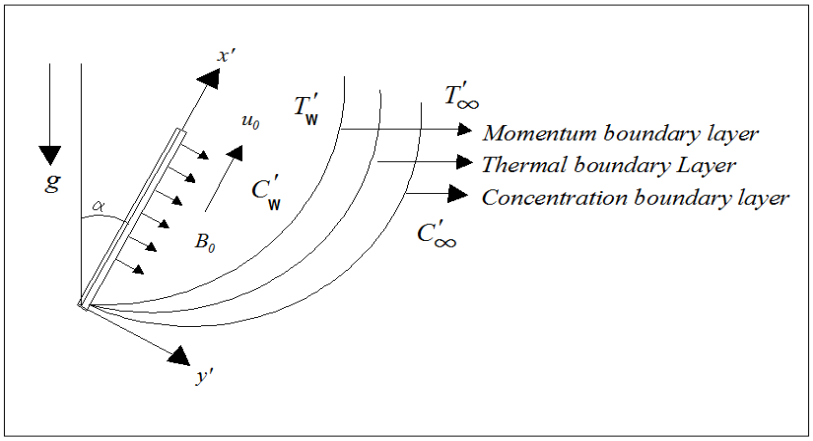

Figure-1. Physical model and coordinate system.

The physical model and coordinates system is shown in Figure-1. pattnaik *et al*. [11] the boundary layer equations of flow, heat and mass transfer past an exponentially accelerated inclined plate are given by

$$\frac{\partial u'}{\partial t'} = g\beta(T' - T'_\infty)\cos\alpha + g\beta'(C' - C'_\infty)\cos\alpha + \nu\frac{\partial^2 u'}{\partial y'^2} - \frac{\sigma B_0^2 u'}{\rho} - \frac{\nu u'}{K'_p} \quad (1)$$

$$\rho c_p \frac{\partial T'}{\partial t'} = k\frac{\partial^2 T'}{\partial^2 y'^2} - \frac{\partial q_r}{\partial y'} + S'(T' - T'_\infty) + \frac{\partial DmK_T}{C_s}\frac{\partial^2 C'}{\partial y'^2} \quad (2)$$

$$\frac{\partial C'}{\partial t'} = D\frac{\partial^2 C'}{\partial y'^2} - K'_c(C' - C'_\infty) + \frac{\rho DmK_T}{T_m}\frac{\partial^2 T'}{\partial y'^2} \quad (3)$$

Initial and boundary conditions are given as:

$$\begin{aligned} &t' \le 0: \ u' = 0, \ T' = T'_\infty, \ C' = C'_\infty \quad for\ all\ y' \\ &t' > 0: \ u' = u_0 \exp(a't'), \ T' = T'_\infty + \frac{(T'_w - T'_\infty)u_0^2 t'}{\nu}, \\ &C' = C'_\infty + \frac{(C'_w - C'_\infty)u_0^2 t'}{\nu} \quad at \quad y' = 0 \\ &and \ \ u' \to 0, \ T' \to T'_\infty, \ \ C' \to C'_\infty \quad as \quad y' \to \infty. \end{aligned} \quad (4)$$

The boundary conditions for the temperature of the plate impose a linearity relation between temperature and time with a residual temperature T'_∞ and having a constant slope $\frac{u_0^2}{\nu}$, which depends upon square of the characteristic velocity and material property. Similar explanation holds for concentration at the plate. The fluid considered here is a gray, absorbing/emitting radiation but a non-scattering medium. The local gradient for the case of an optically thin gray gas is expressed by

$$\frac{\partial q_r}{\partial y'} = -4a^*\sigma(T'^4_\infty - T'^4) \quad (5)$$

We assume that the temperature differences within the flow are sufficiently small and T'^4 can be expressed as a linear function of the temperature. This is accomplished by expanding T'^4 in a Taylor series about T'_∞ and neglecting the higher order terms, we get

$$T'^4 \approx 4T'^3_\infty T' - 3T'^4_\infty. \quad (6)$$

Substitution equations (5) and (6) in equation (2), yields to

$$\rho c_p \frac{\partial T'}{\partial t'} = k\frac{\partial^2 T'}{\partial y'^2} - 16a^*\sigma T'^3_\infty(T' - T'_\infty) + S'(T' - T'_\infty) + \frac{\partial DmK_T}{C_s}\frac{\partial^2 C'}{\partial y'^2} \quad (7)$$

On introducing the following non-dimensional quantities

$$\left.\begin{aligned} &y = \frac{y'u_0}{\nu}, \ U = \frac{u'}{u_0}, \ t = \frac{t'u_0^2}{\nu}, \ a = \frac{a'\nu}{u_0^2}, \ T = \frac{T' - T'_\infty}{T'_w - T'_\infty}, \ C = \frac{C' - C'_\infty}{C'_w - C'_\infty}, \Pr = \frac{\mu c_p}{k}, \\ &Gr = \frac{g\beta\nu(T'_w - T'_\infty)}{u_0^3}, \ Gc = \frac{g\beta'\nu(C'_w - C'_\infty)}{u_0^3}, \ Du = \frac{D_m K_T(C'_w - C'_\infty)}{C_s C_p \nu(T'_w - T'_\infty)}, \ M = \frac{\sigma B_0^2 \nu}{\rho u_0^2}, \\ &Sr = \frac{D_m K_T(T'_w - T'_\infty)}{T_m \nu(C'_w - C'_\infty)}, Kp = \frac{u_0^2 K'_p}{\nu^2}, Kc = \frac{\nu K'_c}{u_0^2}, R = \frac{16a^*\nu^2\sigma T'^3_\infty}{ku_0^2}, S = \frac{s'\nu}{\rho c_p u_0^2}, Sc = \frac{\nu}{D} \end{aligned}\right\} \quad (8)$$

Introducing Equation (9), we obtain non-dimensional form of Equations (2), (8) and (4) respectively:

Equation (1), (7) and (3) reduce to
Momentum equation:

$$\frac{\partial U}{\partial t} = \frac{\partial^2 U}{\partial y^2} - MU - \frac{U}{K_P} + GrT\cos(\alpha) + GcC\cos(\alpha) \quad (9)$$

Energy equation:

$$\frac{\partial T}{\partial t} = \frac{1}{\Pr}\frac{\partial^2 T}{\partial y^2} - \frac{RT}{\Pr} + ST + Du\frac{\partial^2 C}{\partial y^2} \quad (10)$$

Species equation:

$$\frac{\partial C}{\partial t} = \frac{1}{Sc}\frac{\partial^2 C}{\partial y^2} - KcC + Sr\frac{\partial^2 T}{\partial y^2} \quad (11)$$

The corresponding dimensionless boundary conditions are:

$$\left.\begin{aligned} &\{U = 0, \ T = 0, \ C = 0 \quad \forall Y, \quad t \le 0 \\ &\left.\begin{aligned} &U = \exp(at), \ T = t, \ \ C = t \ \ at \ \ y = 0 \\ &U \to 0, \ T \to 0, \ C \to 0, \ as \ \ y \to \infty \end{aligned}\right\} \ \ t > 0 \end{aligned}\right\} \quad (12)$$

Now it is important to calculate the physical quantities of primary interest, which are the local shear stress, local surface heat flux and Sherwood number.

Dimensionless local wall shear stress or skin-friction is obtained as,

$$\tau = \frac{\tau_w}{\rho u_w^2}, \quad \tau_w = \left[\mu \frac{\partial u'}{\partial y'}\right]_{y'=0} = \rho u_o^2 u'(0) = \left[\frac{\partial u}{\partial y}\right]_{y=0} \quad (13)$$

The dimensionless local surface heat flux (i.e., Nusselt number) is obtained as

$$N_u(x') = -\left[\frac{x'}{(T_w' - T_\infty')}\frac{\partial T'}{\partial y'}\right]_{y'=0} \quad \text{then}$$

$$Nu = -\frac{N_u(x')v}{u_0 x'} = -\left[\frac{\partial \theta}{\partial y}\right]_{y=0} \quad (14)$$

The local Sherwood number is obtained as

$$S_h(x') = -\left[\frac{x'}{(C_w' - C_\infty')}\frac{\partial C'}{\partial y'}\right]_{y'=0} \quad \text{then}$$

$$Sh = -\frac{S_h(x')v}{u_0 x'} = -\left[\frac{\partial \phi}{\partial y}\right]_{y=0} \quad (15)$$

Where $R_{e_x} = \frac{u_o x'}{\nu}$ is the Reynold's number.

Method of solution

The finite element method has been implemented to obtain numerical solutions of equations (9)-(11) under boundary conditions (12). This technique is extremely efficient and allows robust solutions of complex coupled, nonlinear multiple degree differential equation systems. The fundamental steps comprising the method are now summarized. An excellent description of finite element formulations is available in Bathe [17] and Reddy [18].

Step-1: Discretization of the Domain into Elements

The whole domain is divided into finite number of sub-domains, a process known as Discretization of the domain. Each sub-domain is termed a finite element. The collection of elements is designated the finite element mesh.

Step-2: Derivation of the element Equations

The derivation of finite element equations *i.e.*, algebraic equations among the unknown parameters of the finite element approximation, involves the following three steps.

a. Construct the variational formulation of the differential equation.
b. Assume the form of the approximate solution over a typical finite element.
c. Derive the finite element equations by substituting the approximate solution into variational formulation.

These steps results in a matrix equation of the form $[K^e]\{u^e\} = \{F^e\}$, which defines the finite element model of the original equation.

Step-3: Assembly of Element Equations

The algebraic equations so obtained are assembled by imposing the "inter-element" continuity conditions. This yields a large number of algebraic equations constituting the "global finite element model", which governs the whole flow domain.

Step-4: Impositions of Boundary Conditions

The physical boundary conditions defined in (12) are imposed on the assembled equations

Step-5: Solution of the Assembled Equations

The final matrix equation can be solved by a direct or indirect (iterative) method.

Grid independence study

To guarantee the grid independent solution a grid refinement test is carried out by dividing the whole domain into successively sized grids *41x41*, *61x61*, and *81x81* in the *y-axis* direction. For all the computations 81 intervals of constant step size 0.01 is considered, which were found to be very accurate. At each node functions are to be evaluated. Hence after assembly of elements a set of 243 non-linear equations are formed, consequently an iterative scheme is adopted and solved by well-known Thomas algorithm. A convergence criterion based on relative difference between two successive iterations was considered and the relative tolerance error has been set to 10^{-5}.

Validation of numerical results

To check the accuracy of the numerical method and code used for the solution of the problem under consideration, it was validated with Pattnaik [11] in the absence of Soret and Dufour effects. This comparison shows good agreement between the results exists. This lends confidence into the numerical results to be reported subsequently.

The above three tables represents the comparison of present values of Skinfriction τ, Nusselt number Nu and Sherwood number Sh with Pattnaik [11]. By observing Table-1 displays the effect of various parameters on Skin friction τ. From this table it is observed that the Skin friction τ increases with increasing the values of M, Sc, Kc, R, α and decreasing the values of Gr, Gc. On the other hand Skin friction τ decreases with increasing the values of Kp, t and

decreasing the values of $\Pr, a$. Table 2 conveys the influence of Prandtl number, heat source parameter, radiation parameter and time on Nusselt number. From this table it is clear that the Nusselt number decreases with decreasing the prandtl number $\Pr$. On the other hand Nusselt number increases on increasing the R, t and decreasing heat source parameter S. Thus it is concluded that the fluid with low thermal diffusivity and higher radiative property favors higher rate of heat transfer at the surface. Table 3 explains the effect of Schmidt number, chemical reaction parameter and time on Sherwood number, it determines the rate of solutal concentration at the surface of the wall. From this table it is clear that Sherwood number increases on increasing Sc , Kc and t. Thus, heavier species with higher rate of chemical reaction increases the rate of solutal concentration at the surface.

Table-1. Comparison of Skin friction τ (when $Sr = 0$ and $Du = 0$).

M	Gr	Gc	Kp	Kc	R	t	Pr	Sc	α	S	a	Pattnaik [11]	Present Results
1	10	5	0.5	0.2	4	0.4	0.71	0.6	π/6	2	0.5	1.2389	1.2389
5	10	5	0.5	0.2	4	0.4	0.71	0.6	π/6	2	0.5	2.3617	2.3617
1	4	5	0.5	0.2	4	0.4	0.71	0.6	π/6	2	0.5	1.6663	1.6663
1	10	0.4	0.5	0.2	4	0.4	0.71	0.6	π/6	2	0.5	1.5951	1.5951
1	10	5	4	0.2	4	0.4	0.71	0.6	π/6	2	0.5	0.7410	0.7410
1	10	5	0.5	2	4	0.4	0.71	0.6	π/6	2	0.5	1.2698	1.2698
1	10	5	0.5	0.2	7	0.4	0.71	0.6	π/6	2	0.5	1.3072	1.3072
1	10	5	0.5	0.2	4	1	0.71	0.6	π/6	2	0.5	-0.5019	-0.5019
1	10	5	0.5	0.2	4	0.4	0.1	0.6	π/6	2	0.5	1.1909	1.1909
1	10	5	0.5	0.2	4	0.4	0.71	3	π/6	2	0.5	1.3503	1.3503
1	10	5	0.5	0.2	4	0.4	0.71	0.6	π/3	2	0.5	1.7036	1.7036
1	10	5	0.5	0.2	4	0.4	0.71	0.6	π/6	0	0.5	1.2742	1.2742
1	10	5	0.5	0.2	4	0.4	0.71	0.6	π/6	2	0.2	0.8947	0.8947

Table-2. Comparison of Nusselt number Nu (when $Sr = 0$ and $Du = 0$).

R	Pr	S	t	Pattnaik [11]	Present Results
4	0.71	2	0.2	0.5214	0.5214
4	0.71	2	0.5	1.0208	1.0208
4	0.5	2	0.2	0.4849	0.4849
10	0.5	2	0.2	0.6832	0.6832
4	0.71	7	0.2	0.4629	0.4629
4	0.71	-2	0.2	0.6145	0.6145

Table-3. Comparison of Sherwood number Sh (when $Sr = 0$ and $Du = 0$).

Sc	Kc	t	Pattnaik [11]	Present Results
0.6	0.2	0.4	0.5674	0.5674
3	0.2	0.4	1.2688	1.2688
0.6	2	0.4	0.6896	0.6896
0.6	0.2	0.8	0.8228	0.8228

RESULTS AND DISCUSSIONS

Comprehensive numerical calculations are performed by using the finite element method to gain a perspective of the flow pattern for various values of the pertinent parameters such as thermal Grashof number, mass Grashof number, magnetic parameter, permeability

parameter, acceleration parameter, Prandtl number, thermal radiation parameter, heat absorption parameter, Dufour number, Schmidt number, Soret number, chemical reaction parameter and time. In the present study we adopted the following default parameter values of finite element computations:

$Gr = 2.0,\ Gc = 2.0,\ M = 2.0,\ K = 0.5,\ \Pr = 0.71,\ R = 4.0,$
$S = 2.0,\ Du = 0.1,\ Sc = 0.6,\ Kc = 0.2,\ Sr = 0.2,$

$t = 0.2$ *and* $\alpha = \frac{\pi}{6}$. All Figures therefore correspond to these values unless specifically indicated on the appropriate figure.

Figure-2 shows the effect of magnetic field parameter M and porosity parameter Kp on velocity profile. For increasing the Magnetic field parameter the velocity will be decreases. This is due to the fact that the introduction of a transverse magnetic field, normal to the flow direction, has a tendency to create the drag known as the Lorentz force which tends to resist the flow. Hence, the horizontal velocity profiles decrease as the magnetic parameter M increases. Similarly, in the case of porosity parameter, if increase the value of Kp then the velocity will be reduces. Figure.3 indicates the effect of angle of inclination α and time t on velocity profile. If increases the angle of inclination and time then velocity increase at all points.

Figure-4 illustrates the effect of heat source parameter and radiation parameter on velocity profile. Clearly observed that an increase in heat source parameter leads to an increase in the velocity. But in case of radiation parameter the reverse effect is observed. Figure-5 exhibits the effect of Schmidt number and chemical reaction parameter on velocity profile. Schmidt number is the ratio of momentum to the mass diffusivity. It is to be found that increase the Schmidt number decreases the velocity and similar effect is observed in case of chemical reaction parameter.

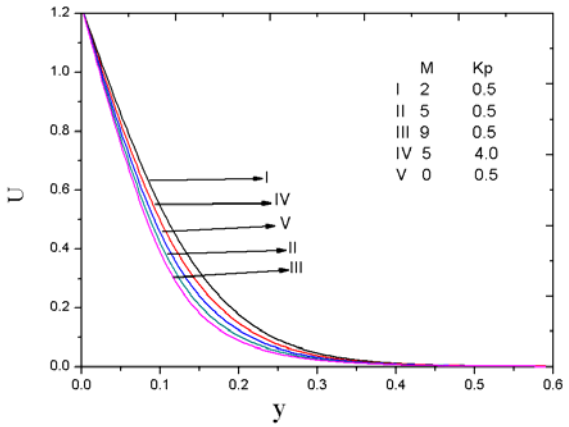

Figure-2. Velocity profile for different M and Kp.

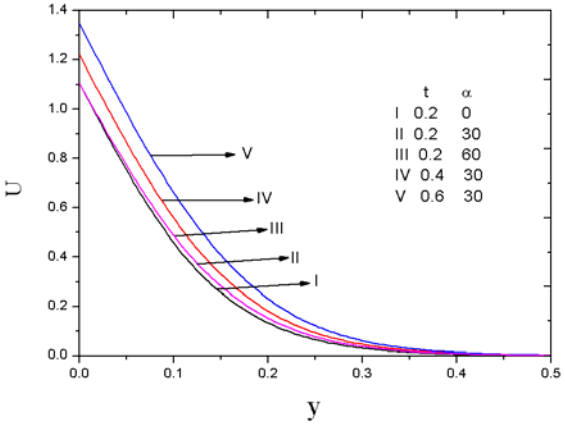

Figure-3. Velocity profile for different t and α.

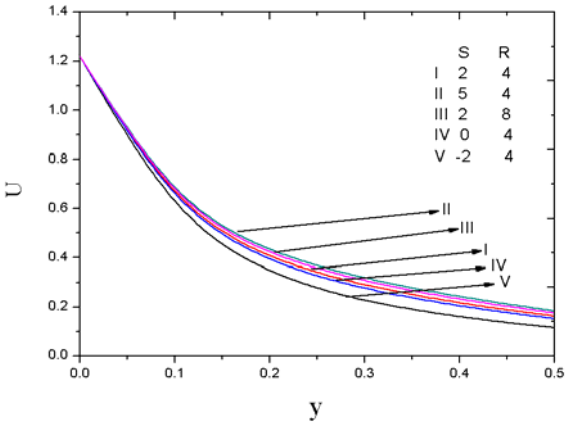

Figure-4. Velocity profile for different S and R.

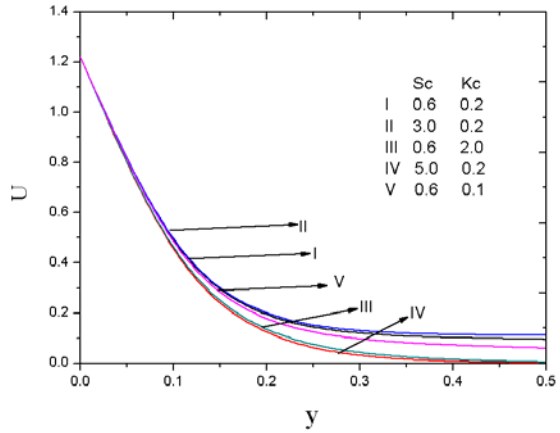

Figure-5. Velocity profile for different Sc and Kc.

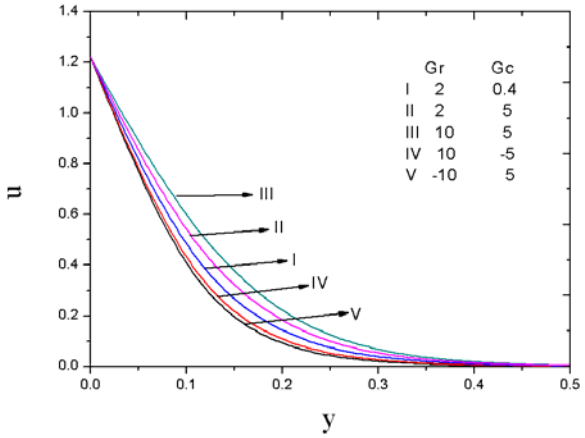

Figure-6. Velocity profile for different Gr and Gc.

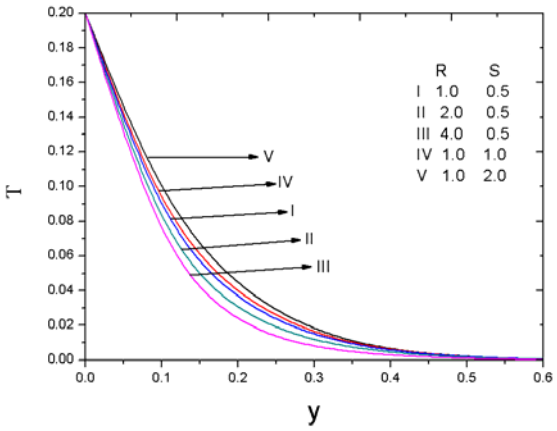

Figure-9. Temperature profile for different R and S.

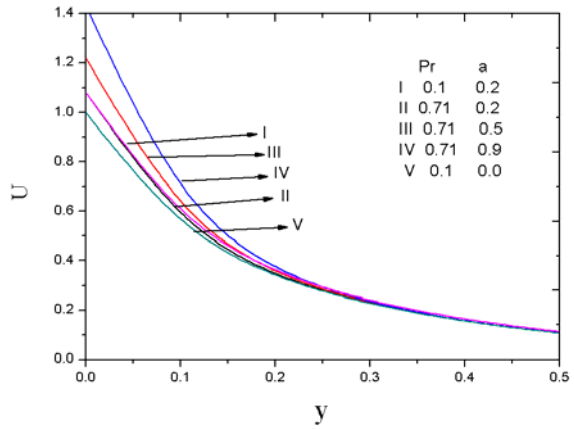

Figure-7. Velocity profile for different Pr and a.

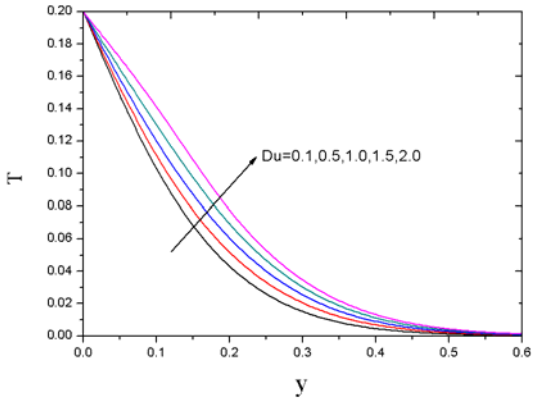

Figure-10. Temperature profile for different Du.

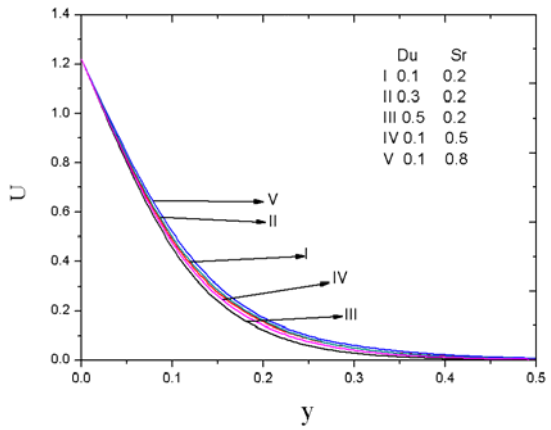

Figure-8. Velocity profile for different Du and Sr.

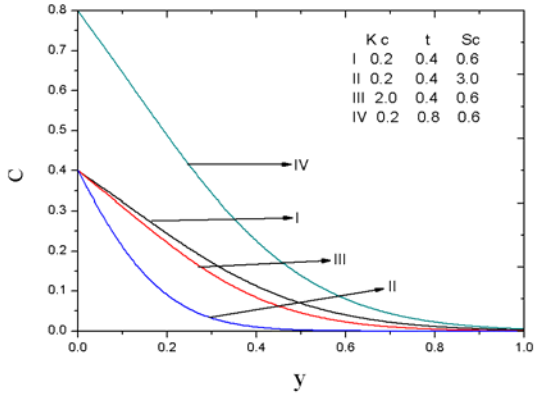

Figure-11. Concentration profile for different Kc, t and Sc.

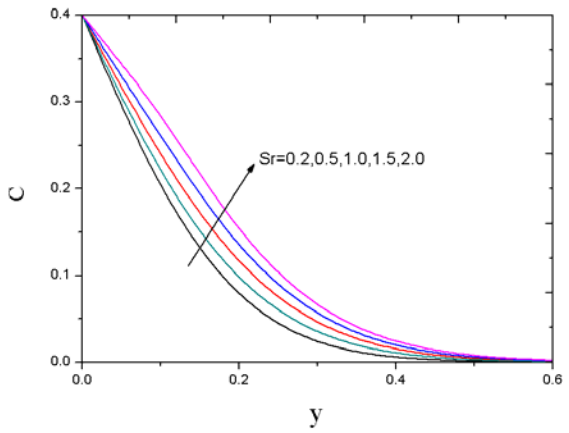

Figure-12. Concentration profile for different Sr .

Figure-6 shows the combined effects of thermal Grashof number Gr and mass Grashof number Gc. The thermal Grashof number Gr signifies the relative effect of the thermal buoyancy (due to density differences) force to the viscous hydrodynamic force in the boundary layer flow. As expected, it is observed that an increase in thermal buoyancy and mass buoyancy leads to the increase in the velocity due to the enhancement in the buoyancy force. Figure-7 indicates the effect of Prandtl number $\Pr$ and acceleration parameter on velocity profile. The Prandtl number defines the ratio of momentum diffusivity to thermal diffusivity. Clearlly observed that an increase in Prandtl number laeds to decrease the velocity and the reverse effect have been observed in case of accelerating parameter.

Figure-8 shows the combined effects of diffusion-thermo and thermal-diffusion. The thermal-diffusion (Soret) effect refers to mass flux produced by a temperature gradient and the diffusion-thermo (Dufour) effect refers to heat flux produced by a concentration gradient. It is found that an increase in the Dufour number and Soret number causes a rise in the velocity throughout the boundary layer.

Figure-9 depict the effect of heat source parameter and radiation parameter on temperature profile. It is noticed that an increase in heat source parameter leads to an increase in the temperature. But in case of radiation parameter the opposite effect have been observed.

For different values of the Dufour number *Du*, the temperature profiles are plotted in Figure-10. The Dufour number *Du* signifies the contribution of the concentration gradients to the thermal energy flux in the flow. It is found that an increase in the Dufour number causes a rise in the temperature throughout the boundary layer. Figure-11 shows that the effect of Schmidt number, time and rate of chemical reaction on concentration profile. The Schmidt number embodies the ratio of the momentum to the mass diffusivity. It is noticed that high value of Sc and higher rate of chemical reaction decreases the concentration at all points. The variation of the concentration distribution of the flow field with the diffusion of the foreign mass is shown in Figure-12. It is observed from this figure that the concentration distribution increases at all points of the flow field with increasing in the Soret number Sr . This shows that the diffusive species with higher value of Soret number have a enhancing effect on the concentration distribution of the flow field.

CONCLUSIONS

In this investigation thermal-diffusion (Soret) and diffusion-thermo (Dufour) effects on MHD flow through porous medium past an exponentially accelerated inclined plate with variable temperature have been developed and then solved numerically by using finite element method. The numerical results are presented graphically and excellent agreement is obtained. Magnetic field parameter M , Porosity parameter Kp , angle of inclination α , Prandtl number $\Pr$, having reverse influence on velocity. Whereas Heat source parameter S , thermal Grashof number Gr , mass Grashof number Gc , and acceleration parameter a having similar influence on velocity. An increase in Heat source parameter S , Dufour effect Du and Soret effect Sr tends to increase in temperature. But in case of radiation parameter R the reverse effect have been observed. Soret number results in an increase in the concentration. Whereas in case of Schmidt number Sc and rate of chemical reaction Kc decreases the concentration.

ACKNOWLEDGEMENTS

The authors are thankful to the University Grants Commission, New Delhi, India for providing financial assistance to carry out this research work under UGC - Major Research Project [F. No. 42 – 22/2013 (SR)].

REFERENCES

[1] Postelnicu A. 2004. Influence of a magnetic field on heat and mass transfer by natural convection from vertical surfaces in porous media considering Soret and Dufour effects. International Journal of Heat and Mass Transfer. 47: 1467-1472.

[2] Ramzan M., S. Saba Inam, A. Shehzad. 2016. Three dimensional boundary layer flow of a viscoelastic nanofluid with Soret and Dufour effects. Alexandria Engineering Journal. 55: 311-319.

[3] Nayak A., S.Panda, D.K Phukan. 2014. Soret and Dufour effects on mixed convection unsteady MHD boundary layer flow over stretching sheet in porous medium with chemically reactive species. Applied Mathematics and Mechanics. 35: 849-862.

[4] Tai Bo-Chen., I. Char Ming. 2010. Soret and Dufour effects on free convection flow of non-Newtonian fluids along a vertical plate embedded in a porous medium with thermal radiation. International Communications in Heat and Mass Transfer. 37: 480-483.

[5] Mohammad Ali., Mohammad Shah Alam.2014. Soret and Hall Effect on MHD flow, heat and mass transfer over a vertical stretching sheet in a porous medium due to heat generation. ARPN Journal of Engineering and Applied Sciences. 9: 361-371.

[6] Seth G.S., R. Sharma, B. Kumbhakar. 2016. Heat and mass transfer effects on unsteady MHD natural convection flow of a chemically reactive and radiating fluid through a porous medium past a moving vertical plate with arbitrary ramped temperature. Journal of Applied and Fluid Mechanics. 9: 103-117.

[7] Siva Reddy Sheri, Suram Anjan Kumar.2016. Finite element analysis of heat and mass transfer past an impulsively moving vertical plate with ramped temperature. Journal of Applied Science and Engineering. 19: 385-392.

[8] Rudraswamy N. G., B. J. Gireesha. 2014. Influence of chemical reaction and thermal radiation on MHD boundary layer flow and heat transfer of a nanofluid over an exponentially stretching sheet. Journal of Applied Mathematics and Physics. 2: 24-32.

[9] Siva Reddy Sheri, Suram Anjan Kumar, Modulgua.Prasanthi.2016. Heat and mass transfer effects on MHD natural convection flow past an infinite inclined plate with ramped temperature. Journal of the Korean Society for Industrial and Applied Mathematics. 20: 355-374.

[10] Anand Rao J., S. Sivaiah, Sk. Nuslin. 2012. Radiation effects on an unsteady MHD vertical porous plate in the presence of homogeneous chemical reaction. ARPN Journal of Engineering and Applied Sciences. 7: 853-859.

[11] Jyotsna Rani Pattnaik., Gouranga charan Dash, Suprava Singh. 2015. Radiation and mass transfer effects on MHD flow through porous medium past an exponentially accelerated inclined plate with variable temperature. Ain Shams Engineering Journal. L, 1-9.

[12] Nield A. Bejan. 1999. Convection in Porous Media, 2nd edition, Springer, New York, USA.

[13] K. Vafai. (Ed.), 2002. Hand Book of Porous Media, vol. II, Marcel Dekker, New York, USA.

[14] Pop D.B., Ingham. 2001. Convective Heat Transfer: Computational and Mathematical of Modeling Viscous Fluids and Porous Media, Pergamon, Oxford.

[15] Das S.S., A. Satapathy, J.K Das, J.P. Panda.2009. Mass transfer effects on MHD flow and heat transfer past a vertical porous plate through a porous medium under oscillatory suction and heat source. International Journal of Heat and Mass Transfer. 52: 5962-5969.

[16] Anand Rao J., S. Sivaiah, R. Srinivasa Raju.2012. Chemical reaction effects on an unsteady magneto hydrodynamics (MHD) free convection fluid flow past a semi-infinite vertical plate embedded in a porous medium with heat absorption. Journal of Applied Fluid Mechanics. 5: 63-70.

[17] Bathe K J. 1996. Finite Element Procedures, Prentice-Hall, New Jersey, USA.

[18] Reddy JN. 2006. An Introduction to the Finite Element Method. McGraw-Hill Book Company: New York, 3rd Edition.